CONF-780892--1

BNL-25311

MASTER

MPS*

S. Ozaki

Brookhaven National Laboratory
Upton, New York 11973

MPS Configuration and Performance Characteristics

The MPS (Multiparticle Spectrometer Facility) is the Laboratory's major spectrometer facility which provides the AGS user community with a comprehensive large aperature spectrometer to carry out their counter physics program at AGS. A schematic layout of the spectrometer which is located in the northwest corner of EEBA is shown in Fig. 1. The main part of the spectrometer is a 700 ton C-magnet with a large field volume (1.82m x 4.55m poles with a 1.21m gap), which is equipped with a set of wire spark chambers giving a good multiparticle handling capability for particle trajectory detection. It also includes a number of proportional chambers and counter hodoscopes to generate a trigger. With a target which is placed in this magnet gap and with a set of target area detectors, a large solid angle coverage ($\sim 4\pi$) to the reaction products can be obtained for an investigation of complex multiparticle final states. The main spectrometer is followed by a set of large spark chambers, scintillation counter hodoscopes and Cerenkov counter hodoscopes for improved momentum resolution and particle identification of those particles which emerge from the MPS magnet. In addition to the basic detectors, the MPS is outfitted with special electronics for trigger logic (RAM), detector readout electronics, data acquisition and recording devices and the on-line computer (PDP10).

The MPS is, at present, serviced by two beams; the MESB from B target station and the HEUB from A target station. The MESB is a medium energy separated beam with a maximum momenta of 10 GeV/c. A good K/π separation can be obtained up to 6 GeV/c and $\bar{p}/\pi$ separation up to the maximum momentum. The HEUB is a high intensity unseparated beam with a maximum momenta of 28.5 GeV/c. The magnet can be rotated around its pivot by $\pm$ 15°. This accommodates MESB and HEUB lines which come from different directions, but also optimizes the detector geometry for some experiments.

DISCLAIMER

At present there are 48 main spark chambers placed in the magnet gap downstream of the target. They are grouped in 8 each of two types of modules, one type being made up of one X, one U, one V, and one X measuring chambers where U and V are ± 15° from the X coordinate, and the other of two Y's. As they are installed in a modular form, the configuration can be altered with relative ease. Both high voltage and ground planes are read out by magnetostrictive lines to give better readout accuracy. The scaler system which encodes these readouts can handle up to 15 sparks for each readout.

The resolving time of the spark chamber system is $\sim$ 2 μsec. This limits the maximum beam flux to $\sim 10^5$/sec. The dead time of the system for clean operation is $\sim$30 msec, thus creating 50% dead time with 15 triggers per AGS pulse. If one takes 3×10^5 particles per AGS pulse incident on 60 cm long hydrogen target, and the trigger rate of 10^{-4}, simple arithmetic gives an attainable sensitivity of 0.4 events/μb/pulse, or 0.5 events/nb/hour. The resolutions of the forward detector system is as follows:

momentum $\quad \frac{\Delta p}{p} \approx \sqrt{(.0025)^2 + (.0012p)^2}$

angular $\quad \Delta\theta_x \approx \frac{3.5 \text{ mr}}{p}$ up to p $\sim$ 7 GeV/c.

Typical effective mass resolutions are:

K^o	4-5 MeV for 0.5 $\sim$ 15 GeV/c
$K^o\pi\pi$ or $K_s^oK_s^o$	20 MeV for 4 GeV mass.

Detector configuration which surrounds the target is expected to be very much experiment-dependent. In fact, with this in mind, the system has been designed to have a maximum flexibility in the area. Currently, two types of detector assembly are available as described below. However, this is the area where the user's imagination and ingenuity will play an important role.

Assembly I: This is a three-sided box made out of modules of plane spark chambers of various sizes which are mounted on a sliding platform. A total of 42 spark chamber gaps are divided into 16 on the right side of the target in four modules, 12 on the downstream in three modules and 14 in the left side in four modules. The readout is by diode-capacitor networks allowing the operation in the magnet gap.

Assembly II: This is a coaxial assembly of 8 cylindrical spark chambers (at present 7 are installed) designed to surround the hydrogen target with the beam passing down the cylinder axis. The chambers are 140 cm long with a diameter which ranges from 33 cm to $\sim$ 100 cm. Each gap is formed by axial wires on the outside and wires spiraling at an angle of 45° to the axis on the inside. The tails of these wires are brought out of the magnetic field for magnetostrictive readout.

Experimental Program at MPS

The MPS has been in operation for the high energy physics research program at the AGS since late 1974. To date it has run five experiments in the MESB beam line and four experiments in the HEUB beam line. A list of the experiments run at the MPS is shown in Table 1. I might add that the program represents the effort made by $\lesssim$ 60 physicists and graduate students from 12 institutions (15 research groups). As can be seen on the Table, the experimental program includes the studies of conventional hadron spectroscopy, the measurement of very small cross section phenomena and the search of new narrow states such as an exotic baryonium state and the charmed particles. This demonstrates the effectiveness and the versatility of the MPS.

In what follows I will discuss some of the experiments which were run in the recent past and those which are scheduled to run in the near future.

1. AGS Experiment 679 (BNL/CCNY)

Limited, but still high data handling capability of the MPS was used to investigate very small cross section phenomena. The reaction studied was:

$$\pi^- p \to \underbrace{K^+K^-}_{\phi} + \underbrace{K^+K^-}_{\phi} + n \qquad \text{at 23 GeV/c}$$

The experiment was run in August-September of 1977 and the preliminary data were published.[1] One of the motivations for this experiment was a search for η_c through its possible decay into $\phi\phi$ final state which is expected to present a low conventional physical background.

Figure 1 shows the way MPS was equipped for this experiment. The trigger was designed to select events with three or more charged kaons produced in a 60-cm-long liquid-hydrogen target. The K-meson signature

was a track emerging from the target with a momentum between 4 and 12 GeV/c, as measured by the proportional wire chambers TPX2 and TPX3 and the counter hodoscope H5, with no signal from the corresponding cell in C6, a Freon 114 threshold-Cerenkov-counter hodoscope. The threshold of C6 for pions was 2.8 GeV/c, and the efficiency was measured to be 99.3% for momenta above 4 GeV/c. Thus, the contamination of pions in the sample is small, although, of course, the counter does not distinguish between kaons and protons. The above selection criteria were achieved using a special trigger system,[2] designed and built at BNL. The system used a fast random-access memory (RAM) with two million bits in a 128 x 128 x 128 three-dimensional array. Each dimension represented one of the three trigger detector elements (TPX2, TPX3, and H5 · $\bar{C}6$). The memory is preloaded to contain "ones" at all three-dimensional points satisfying the chosen criteria. The detector outputs are strobed into a fast register which serves to address the RAM's. 180 nsec later the overall OR tree is strobed to see if any of the addressed combination contains logical "ones".

The hardware is arranged so that the outputs in one dimension are added linearly to give a signal proportional to the number of combinations satisfying the trigger criteria. For this experiment we chose to use H5 · $\bar{C}6$ as this dimension, since at that point the spatial separation between kaons of positive and negative charge is almost complete; by dividing the memory into two sections, we were able to determine the number of particles of each charge. We triggered the spark chambers on events with three or more "kaons" with at least one of each charge. The trigger requirements were satisfied for one in approximately 45,000 incident particles; we recorded 1.3 million triggers. As can be seen in the scatter plot (Fig. 2) of the effective mass of a pair of K^+K^- vs. the other pair of 4-kaon final state, there is a surprisingly clear enhancement of $\phi\phi$ production. The integral of the $\phi\phi$ mass spectra shown in Fig. 3 gives a cross section of 23 ± 2 nb (30% systematic error). The spectrum shows marked enhancement in the low effective mass region but without a clear indication of structure. The upper limit on the σ · BR for η_c, if the mass is $\sim$ 2.8 GeV, is $\sim$ 2 nb.

One thing which is remarkable in our data is a strong enhancement of $\phi\phi$ production which is expected to be OZI suppressed. A comparison

of integrated $\phi\phi$ production cross section with OZI allowed ϕKK production, give a ratio of $\lesssim 10$ (not ~ 100 as one might expect). The other observation made was the enhancement of K^+K^- mass spectra at ϕ mass over background. The degree of the ϕ signal enhancement when the remaining K^+K^- pair is in the ϕ mass band (Fig. 4a) is similar to, if not stronger than that when it is <u>not</u> in the ϕ mass band (Fig. 4b). This certainly is not the behavior one would expect if the $\phi\phi$ production is suppressed by the OZI rule.[3] We therefore have the <u>unusual</u> situation that the "forbidden" reaction produces a higher ϕ enhancement over K^+K^- background than the allowed reaction, although equal enhancements cannot be ruled out because of the possible contamination of the data with $p\bar{p}$ pairs.

The MPS has been active in the searches of exotic states and charmed particles. Two experiments (E686 and E688) were run recently searching for the associated production of charmed particles, and one experiment (E716) was run looking for the exotic baryonium states. The experiment, which is in progress (E682), is also investigating the baryonium states as well as charmed particle production. As the analysis of data from these experiments is not in progress, and the results are not yet available, I can only present how these experiments were run and what one might expect in the results.

2. <u>AGS E686 (Brandeis, BNL, U. Penn., SUNY, Syracuse)</u>

$$\pi^- p \to D^- \;\; C^+$$
$$\hookrightarrow e^- + \text{anything} \quad \hookrightarrow \text{all charged}$$

A pair of transition radiation detectors, which were developed at BNL and located in the MPS gap downstream of the target was used, in conjunction with a shower detector which was located at the downstream exit of the MPS gap for electron identification. The overall hadron rejection ratio of this combination was 1/30K. A good trigger rate of 1/100K was obtained using the electron detectors above and a juditious use of the RAM trigger system mentioned above. Their anticipated sensitivity is such that 20-30 events are expected if the associated production cross section is $\sim$ 100 nb. This assumes the branching ratio for D^- and C^+ to be $\sim$ 10% each.

This experiment also collected extensive data on $\pi^- p \to e^+e^- + X$. The e^+e^- effective mass spectrum which is measured down to the mass

of 20 MeV with an excellent mass resolution inherent to the MPS should prove very significant. They also have data on $e^+e^-\gamma$ to investigate the Dalitz decay of η.

3. AGS E688 (Brandeis, BNL, Cincinnati, Syracuse)

$$\pi^- p \to D^- \quad C^+$$
$$\quad\; \hookrightarrow K^o\mu^-\nu \quad \hookrightarrow \text{all charged}$$

The identification of μ^- was doen using two Cu absorbers with total thickness of $\sim$ 30" placed in the MPS magnet. The increase in the multiplicity gave K^o signature. The sensitivity of the experiment is said to be 1 ev/nb ($\sigma \cdot B$). Therefore, if the $K^o\mu^-\nu$ branching ratio is 10% and $C^+ \to$ all charged branching ratio is 10$\sim$30%, 100 μb associated production cross section should yield $\sim$ 1-3 events.

4. E716 (Carnegie-Mellon, Southeastern Massachusetts University, BNL)

Motivated by the observation of narrow $\bar{p}p$ state at CERN,[4] and encouraged by seeing a possible candidate[5] for this state in their earlier $\bar{p}p$ experiment, this group undertook a search of the exotic baryonium states. The reactions used were:

$$\pi^+ p \to \Delta^o + X^{++} \quad (1)$$
$$\qquad\; \hookrightarrow p\pi^- \quad\; \hookrightarrow \text{reconstructed}$$
$$\to \Delta^{++} + X^o \quad (2)$$
$$\qquad\; \hookrightarrow p\pi^+ \quad\; \hookrightarrow \bar{p}p$$
$$\to \Lambda^o + S^{++} \quad (3)$$
$$\qquad\; \hookrightarrow p\pi^-$$

forward p trigger

$$\pi^+ p \to X^o + \Delta^{++} \quad (4)$$
$$\qquad\; \hookrightarrow \bar{p}p$$
$$\to \bar{p} + (?) \quad (5)$$
$$\qquad\; \hookrightarrow \text{reconstructed}$$

forward $\bar{p}$ trigger

Again the RAM trigger was used to improve the trigger ratio, thus gaining a high sensitivity of the experiment. A post run estimation of the sensitivities of this experiment are:

for $\pi^+ p \to p_{fwd}$ + one or more prongs	$\sim$ 18 ev/nb
for $\pi^+ p \to p_{fwd}$ + 3 or more prongs	$\sim$ 30 ev/nb
for $\pi^+ p \to \bar{p}_{fwd}$ + one or more prongs	$\sim$ 40 ev/nb.

Reactions (1) and (3) are of particular interest. If a narrow resonance peak is observed in the spectrum, it must mean that a manifestingly

exotic state exists which cannot be accommodated by a simple $q\bar{q}$ meson. The sensitivity of the experiment is such that if the narrow $p\bar{p}$ object at 2.2 GeV is produced also in this reaction with cross section of $\sim$ 20 nb, this experiment will see several hundred such events, corresponding to an order of magnitude improvement in the statistics.

5. AGS E682 (Brandeis, BNL, CCNY, U. Mass, SMU)

This is an experiment currently in progress at MPS. One objective of this experiment is to investigate the baryonium production and the other is to search for the charmed particles.

The reactions used for the baryonium study and the expected sensitivities of the experiment are:

$\pi^- p \rightarrow \Delta^o + \bar{p}p$ $\sim$ 30 ev/nb
$\quad \hookrightarrow p\pi^-$ (forward p trigger)

$\pi^- p \rightarrow \Delta^o (p\bar{p}\pi^o)$
$\quad \rightarrow \Delta^o \quad (p\bar{n}\pi^-)$ $\sim$ 2 ev/nb
$\quad \hookrightarrow p\pi^-$ (forward p trigger) $\quad \hookrightarrow$ (side p trigger)

For the charm experiment, the reaction and sensitivity are:

$\pi^- p \rightarrow D^{*-} \quad C^+$
$\quad \hookrightarrow D^o\pi^-$ $\sim$ 20 ev/nb
$\quad\quad \hookrightarrow K^+\pi^-$ (forward K^+ trigger) $\hookrightarrow (\sigma \cdot B)$

6. AGS E705 (CNL, CCNY, Michigan State, Tufts, Vanderbilt)

Another experiment which utilizes the capability of the MPS at its best is the high sensitivity study of the reaction

$\pi^- p \rightarrow V^o V^o$ + neutrals at 23 GeV/c.

This experiment searches for 0^+, 2^+ ... state decay into $K_s^o K_s^o$ and I = 0 state decaying into $\Lambda\bar{\Lambda}$. With anticipated 50 ev/nb sensitivity up to the effective mass of 4 GeV, we expect new interesting features in the mass spectrum which may lead us to an observation of new resonances. A trial run of this experiment was done in conjunction with E679 above. The main run is expected to take place in the Spring of 1979.

MPS Detector Improvement Program

The detector system of the MPS was reviewed recently with an eye toward increased productivity of the spectrometer in the future. Considering the current trend in particle physics which points in the direction of measurements in the sub-nanobarn cross section range, the particle

detectors in the MPS had to be updated with those with higher speed and better spatial resolution. The current spark chamber system can handle only $\sim 10^5$ incident particles per second due to its memory time of $\sim$ 2 μsec limiting the accessible sensitivity to 10-20 nanobarns. The dead time of this new system should be much shorter than the present 30 msec imposed by the spark chambers to reduce the dead time loss of the beam. The present spark chambers operating in the MPS magnetic field suffer from the irreducible systematic error in the position readout due to the ExB shift in the ionization electron from the track.

In order to provide the MPS with such a detector system, a program to develop a suitable drift chamber system with fine cell configuration[6] was started in March of 1978 with an objective to replace the MPS spark chamber system with it in 1980. Initially the system will consist of 3 modules of drift chambers and have 6000 sense wires. The system, upon a successful test, will be expanded to include 10 modules and 20,000 sense wires.

The chambers will be assembled in modules consisting of 5 anode planes. There will be three X measuring (dispersion plane in the MPS) planes XXX' (X' shifted by the anode to field wire spacing). This arrangement permits us to resolve in almost all cases the left-right ambiguity inherent in multi-wire drift chambers. In addition, this arrangement gives a slope and a point for each hit for a majority of cases, giving a significant help for pattern recognition. The other two planes measure the Y coordinate, only one offset Y is used since the trajectory is almost straight in the Y projection permitting several modules to be used to resolve the up-down ambiguity. One of the Y planes has cathode strip readout, where the strips are at $\pm$ 30° to the horizontal; in this way we get three dimensional readout of one avalanche which hopefully will speed up pattern recognition. A configuration of a chamber and the chamber parameters are shown in Fig. 5 and Table 2, respectively.

Figure 6 shows cross sections of a module. The frames are assembled from strips made of a polyester-fiberglass composite,[7] which is formed by pulling the resin fiberglass mixture through a heated die of desired cross section shape in which the material is formed and polmerized. This material has the glass fibers oriented along the pulling

direction, giving an elastic modulus (perpendicular to the pulling direction) 2-3 times that of G-10.

In order to handle signals from as many as 20,000 sense wires and cathode readout strips at an affordable cost, we are presently developing three integrated circuits, i.e. an amplifier, a discriminator and a digital delay-time encoder. These circuits will give us a threshold of approximately 0.5 μamps, ∿ 1 μsec delay for trigger formation, and time digitization with 4 ns time quantization, all at a cost of $6-7/channel in ≥ 100,000 channel quantities.

The amplifier and discriminator are being developed by LeCroy Research Systems, and prototypes are expected sometime next spring. Figure 7 shows the configuration of the amplifier and discriminator. Two different ways of using the discriminator are shown; the first is for straight-forward drift chamber use for application with one discriminator for each readout channel. The second configuration gives three levels of amplitude discrimination for each channel which may be used to measure specific ionization loss, dE/dx. Table 3 summarizes the specifications of the amplifier and discriminator.

The digital delay and time encoder is made from a static 256 bit shift register, which can be clocked at an effective speed of 250 MHz. In this system the clock will keep running, shifting the input from the discriminator continually down the register. When a desired event occurs, the clock will be stopped 256 clock cycle after a time t = 0; the data in a higher segment of the register which contains the time information is read out by restarting the clock at a slower speed. The high speed clock is restarted then to shift in new data. In order to maximize the versatility of the circuit, the length of the segment that can be read out will be controlled by an external device and could, if desired, include the entire register. This circuit is being built by RCA using CMOS/SOS technology which offers high speed, low power consumption, high density, and low cost; prototype delivery is approximately one year. CMOS/SOS is not presently capable of operating at 250 MHz. We, therefore have resorted to use a four-phase clock at 62.5 MHz, clocking four 64 bit shift registers each having 90° relative phase shift. Readout speed is restricted by the ability of the output device

to drive a capacitive load to approximately 25 MHz. Table 4 summarizes the specifications of the digital delay. Figure 8a shows the logic diagram for a single channel; Figure 8b is the diagram for a package. Only 2 clocks are drawn because $C_3 = \bar{C}_1$ and $C_4 = \bar{C}_2$. An open drain (or its equivalent) output will be used so that several packages (up to 32) can be wire or'ed together for readout.

In the MPS system we expect to have a readout controller for each group of 500 wires, which when reading out 32 bits/wire at 25 million bits/second with all controllers operating in parallel gives a total readout time of 650 μs. These controllers will initialize the system by setting the enable controls so that all channels can read in data and turn on the fast clocks. When a preliminary trigger is generated, the controller will stop the fast clocks, holding the data until a final trigger is formed and the readout cycle started. A readout cycle consists of resetting all the enable controls, shifting a one into the first enable control shift register and starting the readout clock, which reads out the first channel. When the desired number of bits (32 for the MPS) have been read from the first channel, encoded and stored in cache memory, the one is shifted to the next channel, enabling the readout of channel 2; this process is repeated until all channels in a given subsystem have been read into the controller. Data from the cache memory is transferred to main data storage, and the system is ready to be reinitialized. If, on the other hand, no final trigger was formed, the fast clock would be restarted.

The anticipated performance characteristics of the new drift chamber detector system are compared to those for the current spark chamber system and are shown in Table 4. It is clear that the new system will have more than an order of magnitude improvement in the resolving time, giving like improvement in the beam rate handling capability. A much shorter dead time will give us a capability to collect the data at a higher rate without significant dead time loss of the beam. The improvement of the spatial resolution by more than a factor of two is important particularly for a search of narrow objects.

We are looking forward to the new kind of spectroscopy and study of hadron dynamics with the new MPS detectors.

* Work performed under Contract No. EY-76-C-02-0016 with the Department of Energy.

REFERENCES

1. A. Etkin, K.J. Foley, J.H. Goldman, W.A. Love, T.W. Morris, S. Ozaki, E.D. Platner, A.C. Saulys, C.D. Wheeler, E.H. Willen, S.J. Lindenbaum, M.A. Kramer and U. Mallik, Phys. Rev. Lett. 40, 422-425 (1978).
2. E.D. Platner, A. Etkin, K.J. Foley, J.H. Goldman, W.A. Love, T.W. Morris, S. Ozaki, A.C. Saulys, C.D. Wheeler, E.H. Willen, S.J. Lindenbaum, J.R. Bensinger and M.A. Kramer, Nucl. Instr. and Methods 140, 549 (1977).
3. A. Etkin, K.J. Foley, J.H. Goldman, W.A. Love, T.W. Morris, S. Ozaki, E.D. Platner, A.C. Saulys, C.D. Wheeler, E.H. Willen, S.J. Lindenbaum, M.A. Kramer and U. Mallik , Phys. Rev. Lett. 41, 784 (1978).
4. P. Benkheiri et al., Phys. Lett. 65B, 483 (1977).
5. Search for Narrow States in $\bar{p}p \to \pi^+(\pi^-K^+K^-)$ at 6 and 8 GeV/c, Carnegie-Mellon University, Southeastern Massachusetts University, University of Massachusetts Collaboration (Paper #810) Contribution to the XIX Int. Conf. on High Energy Physics, 23-31 August 1978, Tokyo, Japan.
5. E.D. Platner, IEEE Transactions on Nuclear Science, Vol. NS-25, No. 1, February 1978, p. 35.
6. A. Etkin, A Drift Chamber System for Use in a High Rate Environment, Contribution to the 1978 Nuclear Science Symposium, October 18-20, 1978, to be published. BNL 24624.

TABLE 1

	E654	Brandeis, BNL, CMU, Cincinnati, CCNY, U. Mass, U. Penn, SMU, Syracuse	$\bar{p}p \rightarrow \bar{\Lambda}\Lambda$ (η_c search)	††	MESB	4 GeV/c $\bar{p}$
December	E557	Brandeis, BNL, CCNY, U. Mass, U. Penn	$K^-p \rightarrow K^{*}n$ $\rightarrow K^-\pi^+$	††	MESB	6 GeV/c K^-
1976 January	E594	BNL, CCNY	$K^-p \rightarrow K^{*}n$ $\rightarrow K^o\pi^+\pi^-$	††	MESB	6 GeV/c K^-
February						
March April	E601	Brandeis, Cincinnati, Syracuse	$\bar{p}p \rightarrow \bar{\Lambda}\Lambda$ $\rightarrow \bar{p} + \pi^+$	††	MESB	3 GeV/c $\bar{p}$
May June July August	Test					
September October November December	E596	Carnegie-Mellon, SE Massachusetts U.	$\bar{p}p \rightarrow \pi^-\pi^+$, $\pi^+p \rightarrow p\pi^+$ $\bar{p}p \rightarrow \pi^+\pi^-$, $\pi^-p \rightarrow p\pi^-$ $\bar{p}p \rightarrow \pi^+\rho$, $\pi^-p \rightarrow p\rho^-$	†† †† ††	MESB	4,6,8 GeV/c $\bar{p}$
1977 January	Test					
February March April May						
June	Test					
July August September	E679	BNL,CCNY	$\pi^-p \rightarrow \phi\phi + X^o$ ϕK, ϕ, $\pi + X$ $K^+K + X$ etc.	††	HEUB	23 GeV/c π^-

Table 2

Drift Distance	0.125"
Anode to Cathode Distance	0.250"
Anode Wire	0.001" Dia. Tungsten, Gold Plated
Field Wire	0.003" Dia. Nitronic-50 Stainless Steel
Cathode Wire	0.003" Dia. Nitronic-50 Stainless Steel (20/in.)
Frame Material	Pultrusion, Polyester Fiberglass (Composite)

Table 3

Number of Channels/package	- 4
Amplifier Transresistance	- 50 KΩ
Input Impedance	- < 50Ω
Input Noise	- < 0.25 μa rms
Risetime	- < 4 ns
Overload Recovery	- < 40 ns for 30 ns wide 100 μA pulse
Input protection	- discharge of 100 pf capacitor charged to 3 KV
Discriminator time slewing	- < 4 ns for 2X-20X threshold
Hysteresis	- 6 mv
Threshold	- 0 to 500 mv
Threshold match	- ± 5 mv
Crosstalk between channels	- > 40 db down
Output	- low: 1.5 volt high: 3.5 volt 3 ns risetime

Table 4

Channel/package	- 4
Maximum clock speed	- > 65 MHz
Maximum readout speed	- > 20 MHz
Data setup time variation within a channel	- ± 1 ns
Data Input	- Differential
Clock Input	- C_1, $\bar{C}_1$, C_2, $\bar{C}_2$
Logic Levels (except data)	- Low 0.5 ± 0.5 volts High 4.5 ± 0.5 volts
Data Logic Levels	- Low - 1.5 volts High - 3.5 volts

Table 5

	Spark Chamber	Drift Chamber
Resolving time	2 μsec ↳ memory time	∿ 60 μsec ↳ max. drift. time
Dead time	30 msec ↳ clearing	∿ 1 msec ↳ data encoding
Spatial resolution	∿ 800 μ ↳ limited by ExB shift	100-200 μ ↳ geometrical alignment
Pattern recognition	Point assembly	Segment assembly

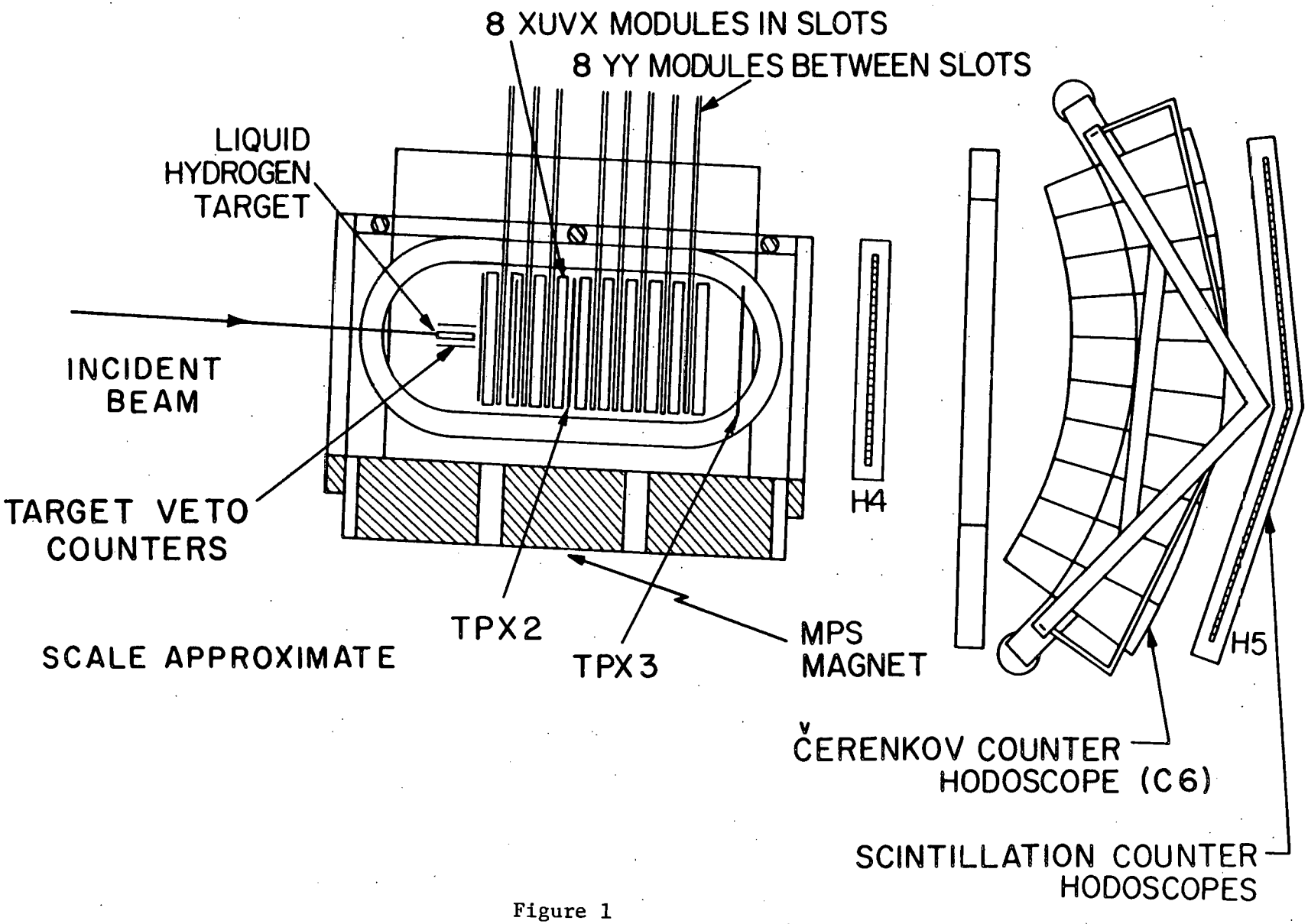
8 XUVX MODULES IN SLOTS
8 YY MODULES BETWEEN SLOTS
LIQUID HYDROGEN TARGET
INCIDENT BEAM
TARGET VETO COUNTERS
SCALE APPROXIMATE
TPX2
TPX3
MPS MAGNET
H4
H5
ČERENKOV COUNTER HODOSCOPE (C6)
SCINTILLATION COUNTER HODOSCOPES

Figure 1

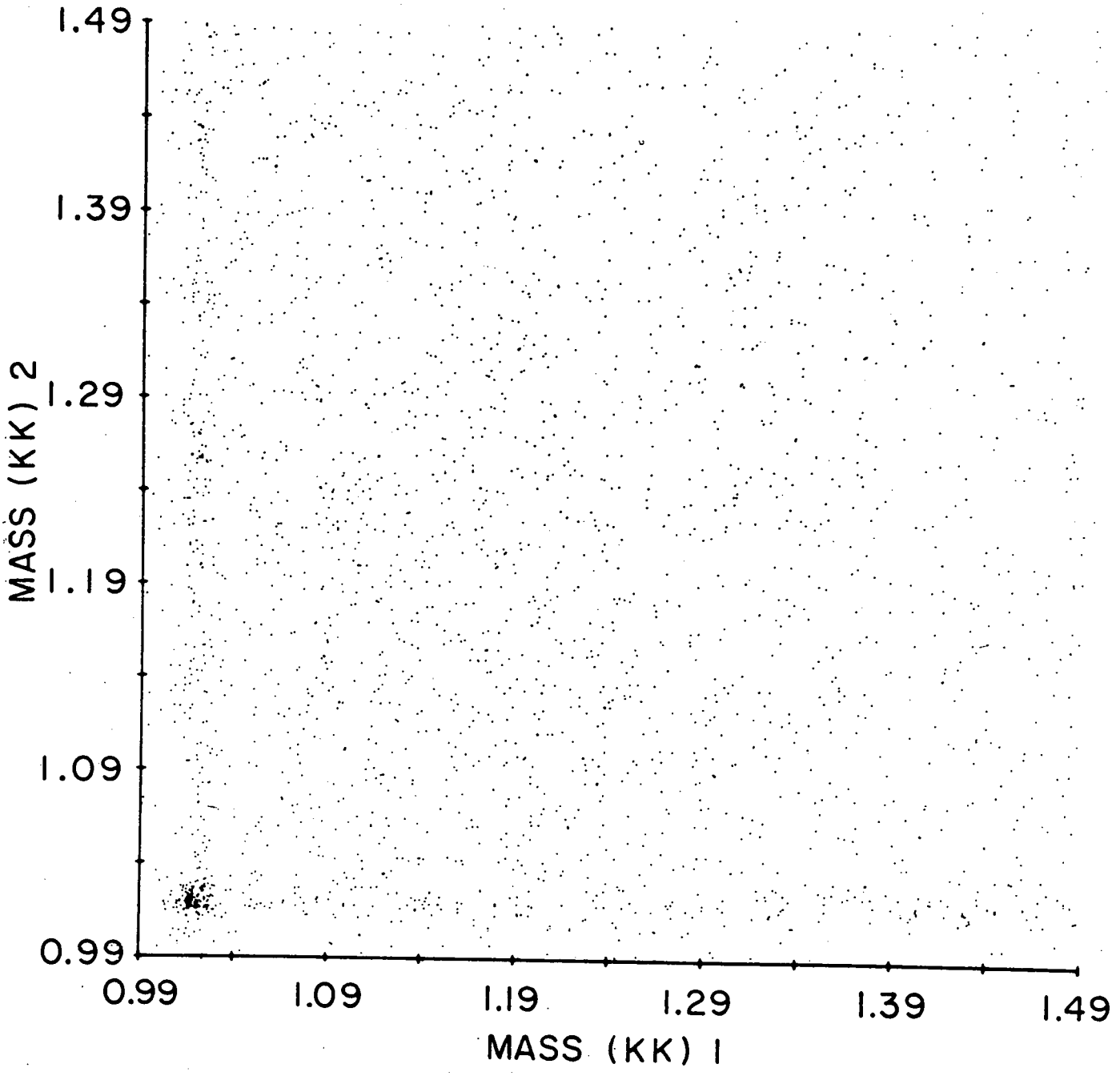
1.49
1.39
1.29
1.19
1.09
0.99
MASS (KK) 2
0.99
1.09
1.19
1.29
1.39
1.49
MASS (KK) 1

Figure 2

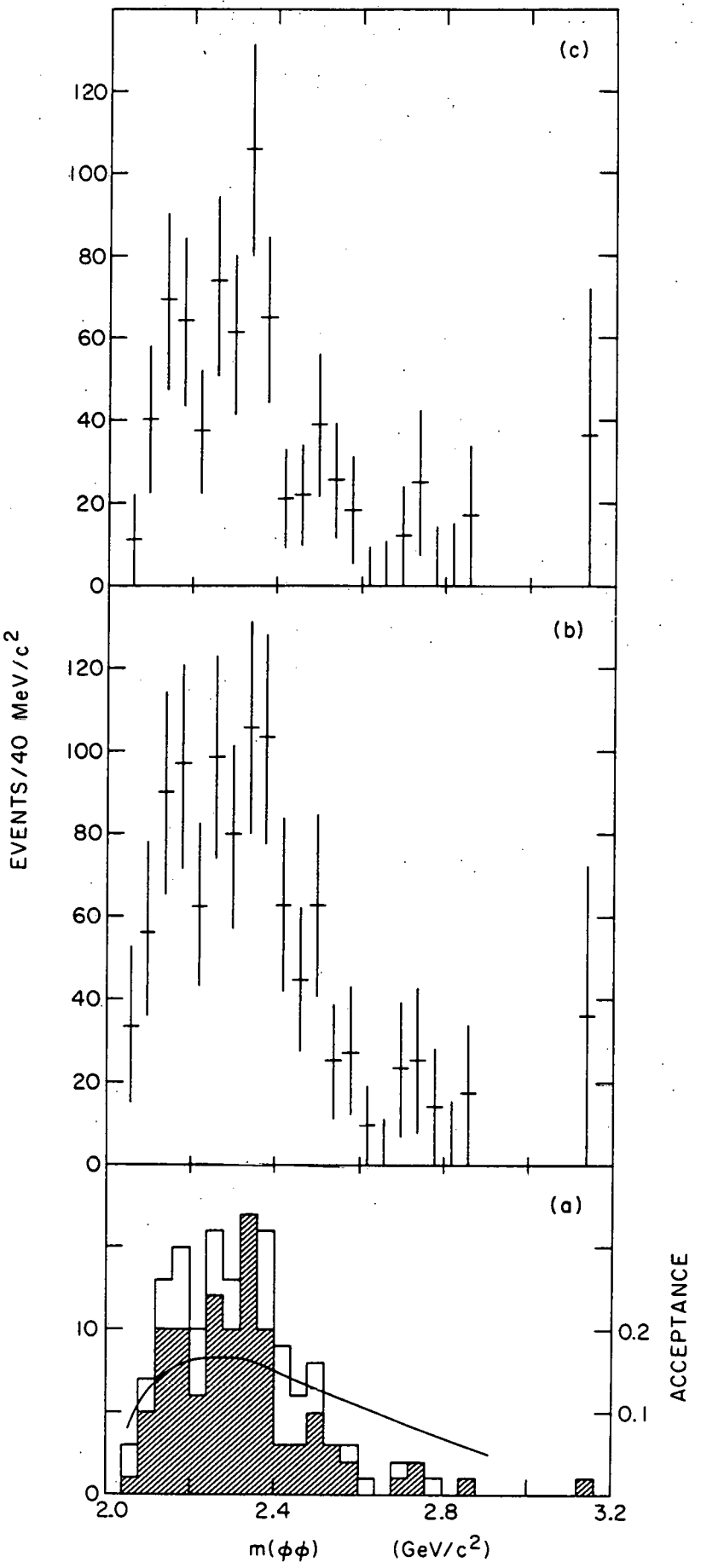
(c)
(b)
(a)
EVENTS/40 MeV/c²
ACCEPTANCE
m(φφ) (GeV/c²)
0
20
40
60
80
100
120
10
0.1
0.2
2.0
2.4
2.8
3.2

Figure 3

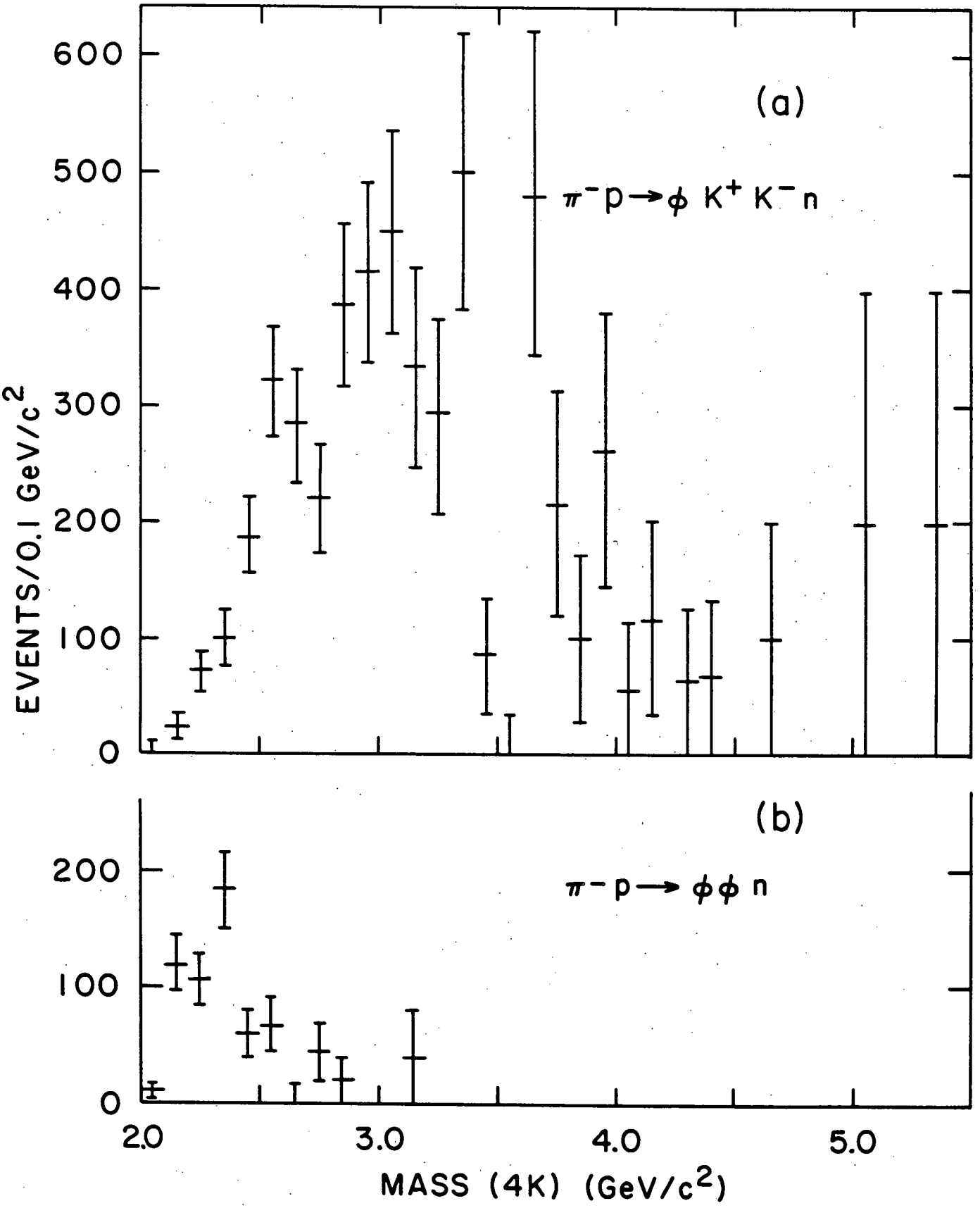
(a)
$\pi^- p \to \phi K^+ K^- n$
EVENTS/0.1 GeV/c^2
600
500
400
300
200
100
0
(b)
$\pi^- p \to \phi\phi n$
200
100
0
2.0
3.0
4.0
5.0
MASS (4K) (GeV/c^2)

Figure 4

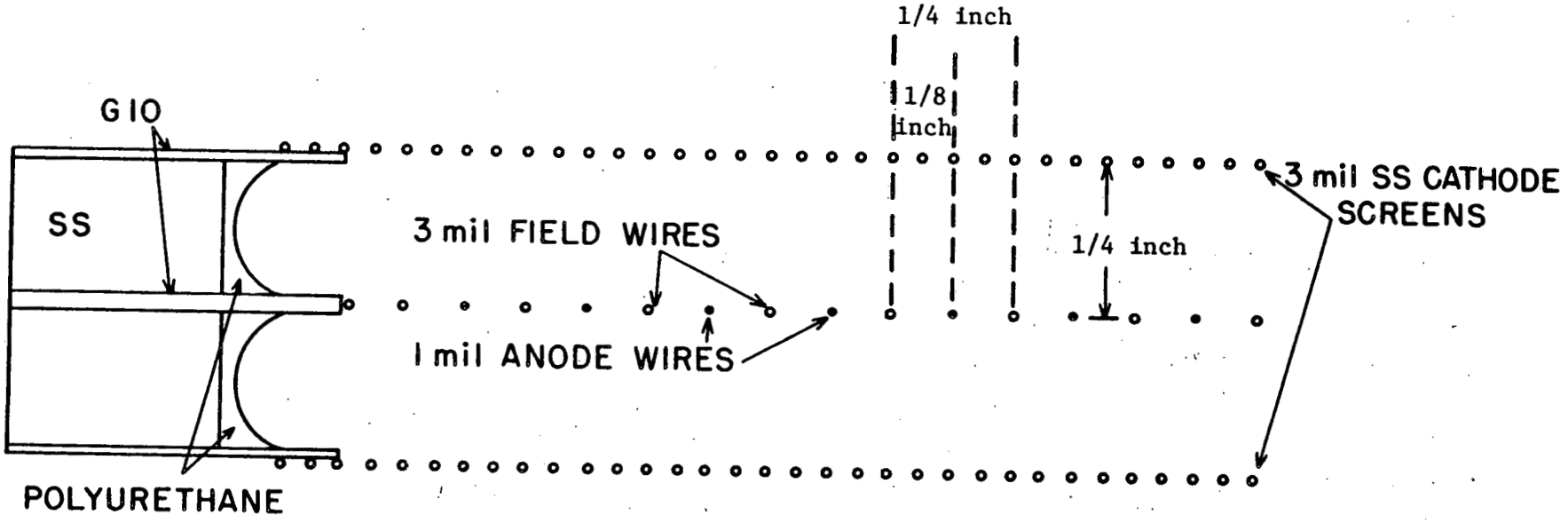

DRIFT PROPORTIONAL WIRE CHAMBER

Figure 5

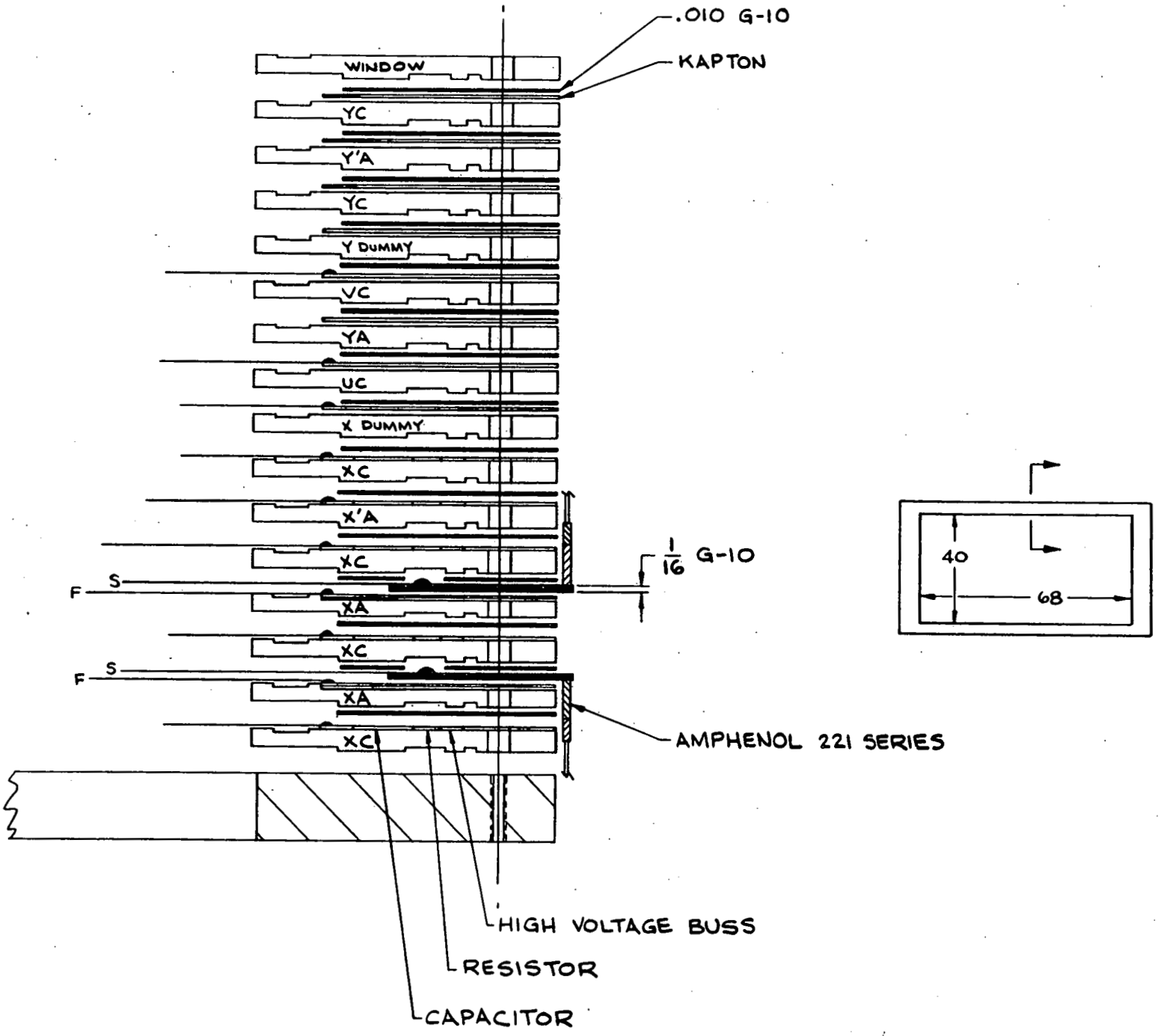
.010 G-10
KAPTON
WINDOW
YC
Y'A
YC
Y DUMMY
VC
YA
UC
X DUMMY
XC
X'A
XC
S
F
XA
XC
S
F
XA
XC
1/16 G-10
AMPHENOL 221 SERIES
HIGH VOLTAGE BUSS
RESISTOR
CAPACITOR
40
68

Figure 6a

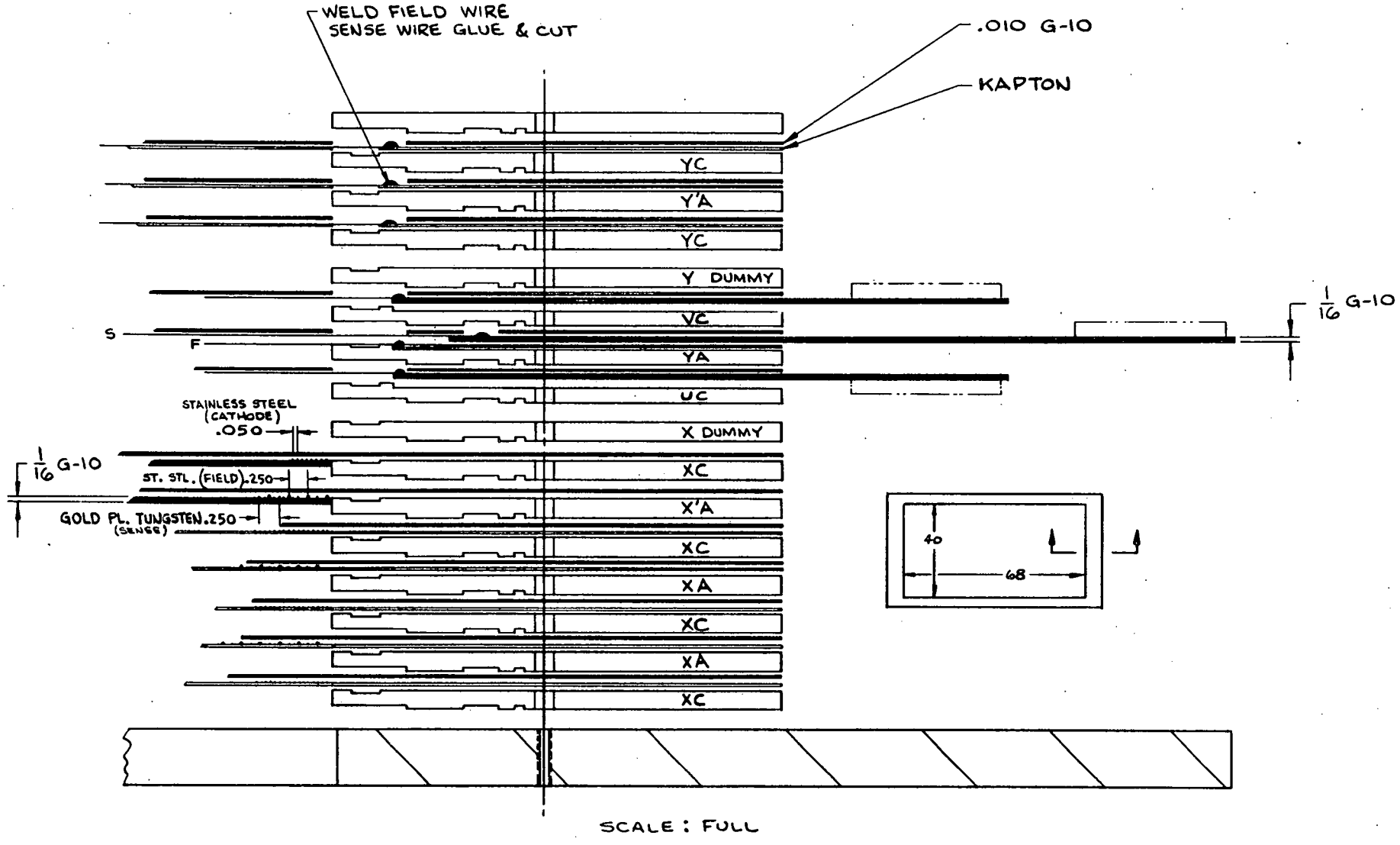
WELD FIELD WIRE
SENSE WIRE GLUE & CUT
.010 G-10
KAPTON
YC
Y'A
YC
Y DUMMY
VC
YA
UC
X DUMMY
XC
X'A
XC
XA
XC
XA
XC
S
F
1/16 G-10
STAINLESS STEEL (CATHODE) .050
1/16 G-10
ST. STL. (FIELD) .250
GOLD PL. TUNGSTEN .250 (SENSE)
40
68
SCALE : FULL

Figure 6b

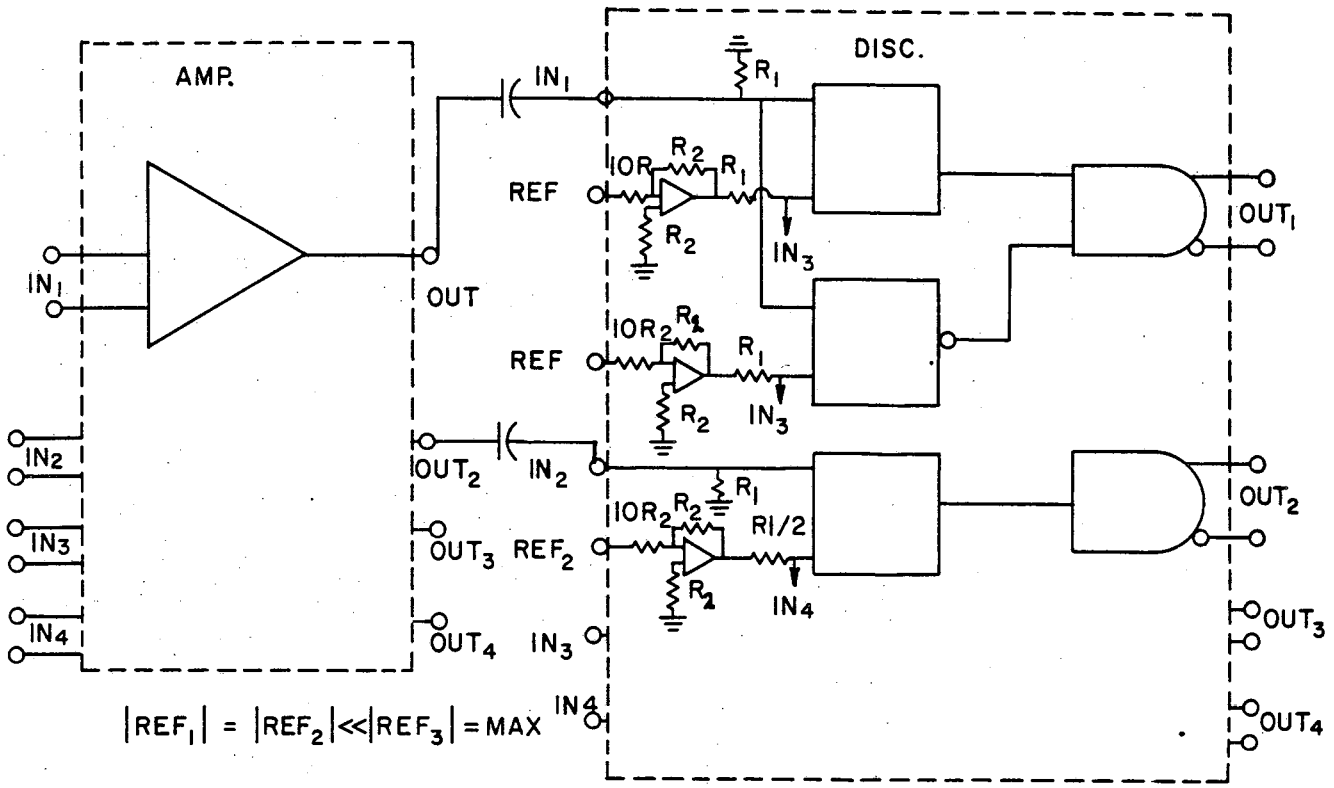
AMP.
DISC.
IN1
OUT
IN2
IN3
IN4
OUT2
OUT3
OUT4
R1
R2
10R
REF
IN3
R1/2
REF2
IN4
OUT1
|REF1| = |REF2|<<|REF3| = MAX

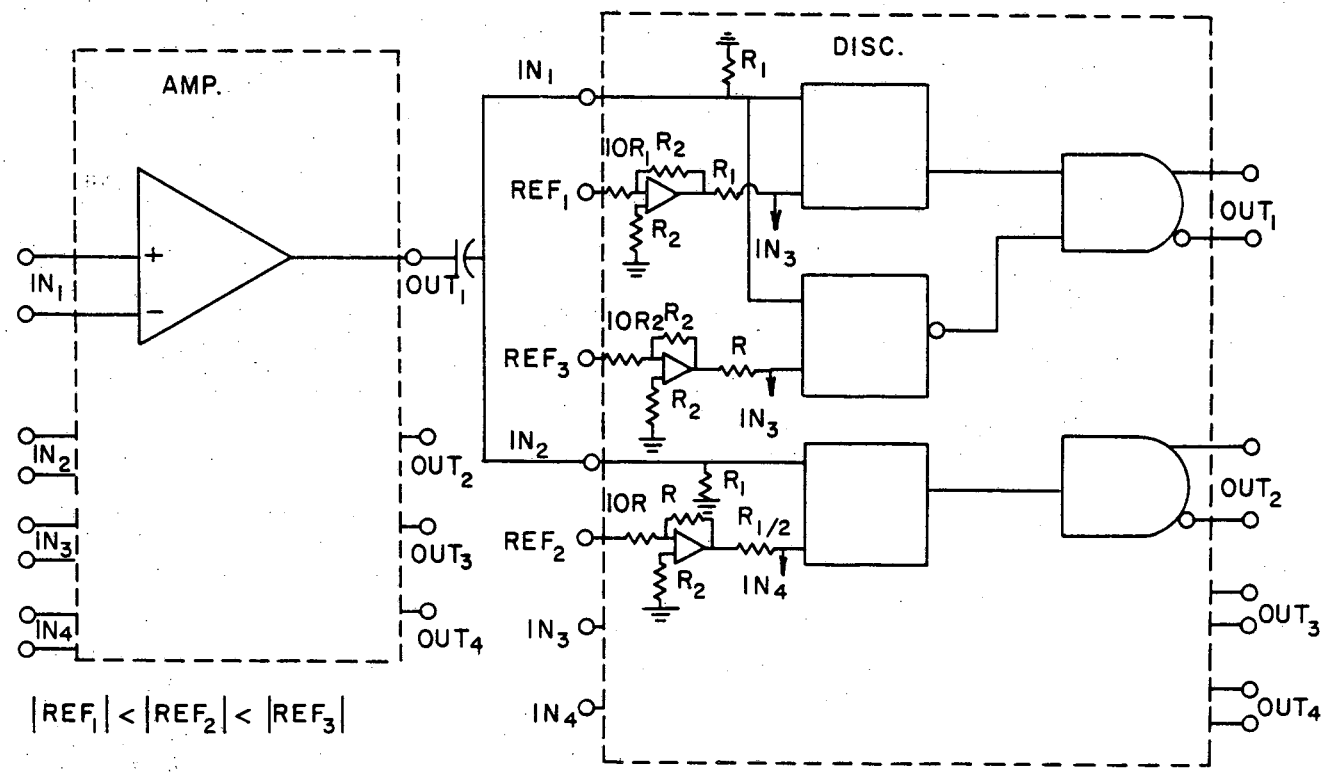
AMP.
DISC.
IN1
OUT1
IN2
IN3
IN4
OUT2
OUT3
OUT4
R1
R2
10R1
REF1
10R2
REF3
R
10R
REF2
R1/2
IN3
IN4
|REF1| < |REF2| < |REF3|

Figure 7

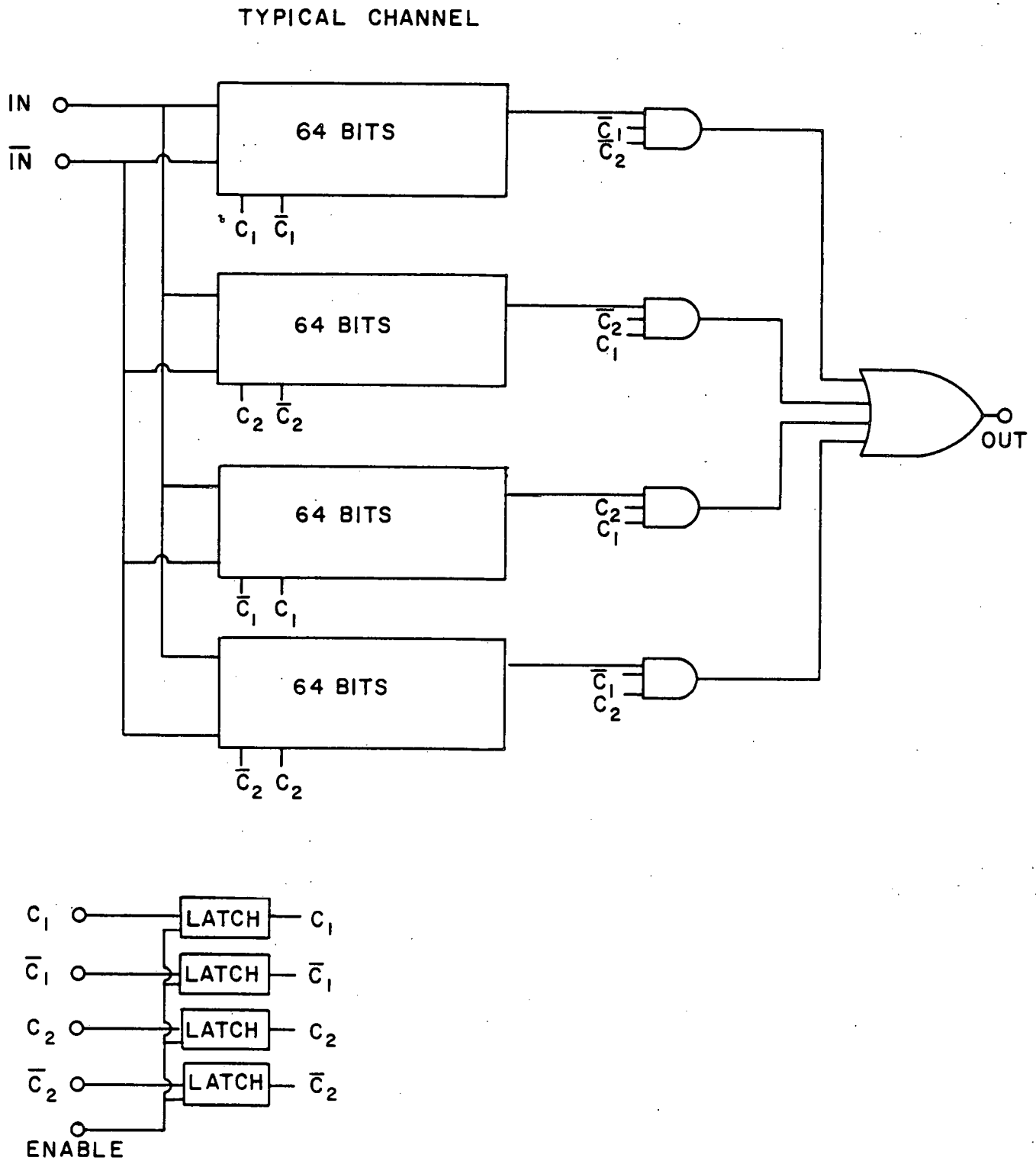
TYPICAL CHANNEL
IN
$\overline{IN}$
64 BITS
64 BITS
64 BITS
64 BITS
C_1 $\overline{C}_1$
$\overline{C}_2$ C_2
$\overline{C}_1$ C_1
C_2 $\overline{C}_2$
$\overline{C}_1$ $\overline{C}_2$
C_2 C_1
$\overline{C}_2$ C_1
$\overline{C}_1$ C_2
OUT
C_1
$\overline{C}_1$
C_2
$\overline{C}_2$
ENABLE
LATCH
LATCH
LATCH
LATCH
C_1
$\overline{C}_1$
C_2
$\overline{C}_2$

Figure 8a

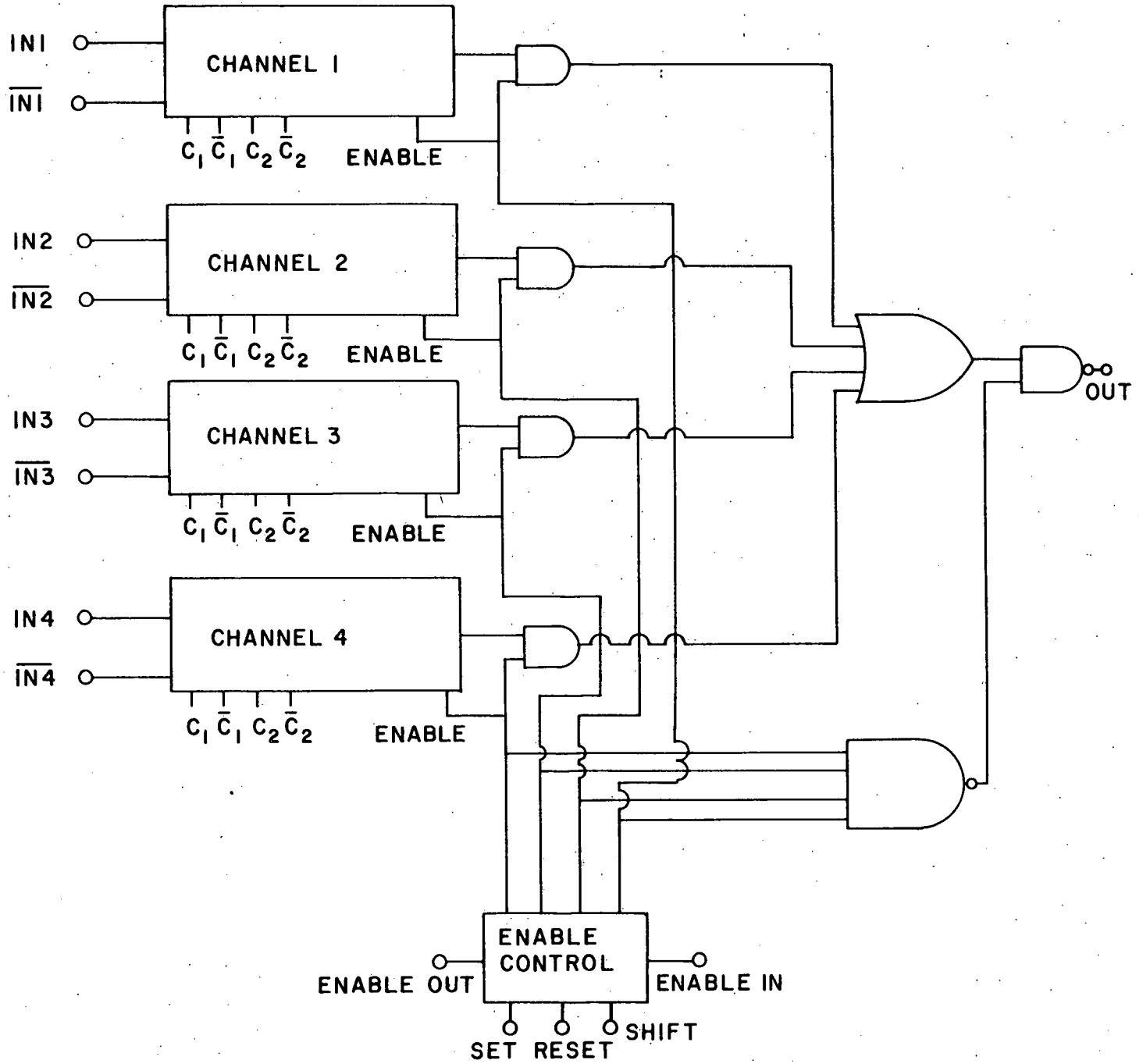
IN1
$\overline{IN1}$
CHANNEL 1
C_1 $\bar{C}_1$ C_2 $\bar{C}_2$
ENABLE
IN2
$\overline{IN2}$
CHANNEL 2
C_1 $\bar{C}_1$ C_2 $\bar{C}_2$
ENABLE
IN3
$\overline{IN3}$
CHANNEL 3
C_1 $\bar{C}_1$ C_2 $\bar{C}_2$
ENABLE
IN4
$\overline{IN4}$
CHANNEL 4
C_1 $\bar{C}_1$ C_2 $\bar{C}_2$
ENABLE
OUT
ENABLE CONTROL
ENABLE OUT
ENABLE IN
SET
RESET
SHIFT

Figure 8b